HHS Public Access

Author manuscript

Nat Genet. Author manuscript; available in PMC 2012 March 01.

Published in final edited form as:

Nat Genet. ; 43(9): 854–859. doi:10.1038/ng.905.

MicroRNAs can generate thresholds in target gene expression

Shankar Mukherji[1,7], **Margaret S. Ebert**[2,3,7], **Grace X. Zheng**[2,4], **John S. Tsang**[6], **Phillip A. Sharp**[2,3], and **Alexander van Oudenaarden**[2,3,5]

[1]Harvard-MIT Division of Health Sciences and Technology, Massachusetts Institute of Technology, Cambridge, MA 02139, USA

[2]Koch Institute for Integrative Cancer Research, Massachusetts Institute of Technology, Cambridge, MA 02139, USA

[3]Department of Biology, Massachusetts Institute of Technology, Cambridge, MA 02139, USA

[4]Computational and Systems Biology Graduate Program, Massachusetts Institute of Technology, Cambridge, Massachusetts 02139, USA

[5]Department of Physics, Massachusetts Institute of Technology, Cambridge, MA 02139, USA

[6]Graduate Program in Biophysics, Harvard University, Cambridge, MA, 02138, USA

Abstract

MicroRNAs (miRNAs) are short, highly conserved non-coding RNA molecules that repress gene expression in a sequence-dependent manner. We performed single-cell measurements using quantitative fluorescence microscopy and flow cytometry to monitor a target gene's protein expression in the presence and absence of regulation by miRNA. We find that while the average level of repression is modest, in agreement with previous population-based measurements, the repression among individual cells varies dramatically. In particular, we show that regulation by miRNAs establishes a threshold level of target messenger RNA (mRNA) below which protein production is highly repressed. Near this threshold, protein expression responds sensitively to target mRNA input, consistent with a mathematical model of molecular titration. These results demonstrate that miRNAs can act both as a switch and as a fine-tuner of gene expression.

MicroRNAs regulate protein synthesis in the cell cytoplasm by promoting target mRNAs' degradation and/or inhibiting their translation. Their importance is suggested by the predictions that each miRNA targets hundreds of genes and that the majority of protein-coding genes are miRNA targets[1–4]; by their abundance, with some miRNAs expressed as high as 50,000 copies per cell[5]; and by their sequence conservation, with some miRNAs conserved from sea urchins to humans[6]. miRNAs can regulate a large variety of cellular

Correspondence should be addressed to A.v.O. (avano@mit.edu).

[7]These authors contributed equally to this work.

AUTHOR CONTRIBUTIONS

M.S.E., J.S.T., P.A.S. and A.v.O. conceived the project. M.S.E., S.M. and G.X.Z. performed the experiments. S.M. and M.S.E. processed the data and constructed the model; S.M. quantitatively analyzed the model. S.M., M.S.E., A.v.O. and P.A.S. interpreted the results and wrote the paper.

processes, from differentiation and proliferation to apoptosis[7–11]. miRNAs also confer robustness to systems by stabilizing gene expression during stress and in developmental transitions[12,13].

Despite the evidence for the importance of gene regulation by miRNAs, the typical magnitude of observed repression by miRNAs is relatively small[2,3], with some notable exceptions such as the switch-like transitions due to miRNAs *lin-4* and *let-7* targeting the heterochronic genes *lin-14* and *lin-41* respectively in *Caenorhabditis elegans*[14]. Importantly however, most of the previous studies of regulation by miRNAs in mammalian cells have measured population averages, which often obscure how individual cells respond to signals[15].

In our study, we aim to complement previous work demonstrating the breadth and importance of gene regulation by miRNA by directly measuring the effects of miRNA on target gene expression in single cells. Through the use of a two-color fluorescent reporter system that allows us to simultaneously track gene expression in the presence and absence of binding sites for miRNA, we are able to measure both transcription and translation following regulation by miRNA in single mammalian cells. Our single-cell analysis revealed two unexpected features. First, the experiments showed that regulation by miRNA imposes a previously unappreciated nonlinearity relating target transcript abundance to target protein abundance; namely, target protein production is highly repressed below a threshold level of target mRNA production and responds sensitively to transcription above this threshold. Second, there is considerable cell-to-cell variability in the strength of repression in a population of identically prepared cells. Most notably, the fold repression of miRNA targets below the threshold can be far greater than measured for the population average, up to 40-fold in our data. Motivated by previous work on protein-protein interactions[16–17] and regulation by bacterial small RNA[18] (sRNA), we employed and experimentally tested a mathematical model to formally describe the biochemical interactions comprising the miRNA regulatory system. The model suggested the importance of molecular titration in generating the sensitive response to transcription above the threshold. In this picture, as target abundance increases, target mRNAs titrate away the pool of miRNAs available for repression; the sharpness of the switch from full repression to escape from miRNA repression depends on the strength of the interaction between miRNA and target as well as their relative abundances.

RESULTS

Quantitative single-cell fluorescence microscopy reveals microRNA-mediated gene expression thresholds

To assay for miRNA activity in single mammalian cells, we constructed a two-color fluorescent reporter system that permits simultaneous monitoring of protein levels in the presence and absence of regulation by miRNA (Fig. 1a). The construct consists of a bidirectional Tet-inducible promoter driving two genes expressing the fluorescent proteins mCherry and eYFP tagged with nuclear localization sequences. The 3′ UTR of mCherry is engineered to contain *N* binding sites for miRNA regulation. In the first set of experiments, the inserted sites are recognized by miR-20, which is expressed endogenously in HeLa cells

along with its seed family members miR-17-5p and miR-106b. The 3′ UTR of eYFP is left unchanged so that it can serve as a reporter of the transcriptional activity in a single cell.

We constructed cell lines that stably expressed the fluorescent reporter construct with either a single bulged miR-20 binding site or no site in the mCherry 3′ UTR. The levels of eYFP and mCherry protein were measured in single cells using quantitative fluorescence microscopy. Arranging individual cells according to their eYFP expression level, we observed that cells whose mCherry 3′ UTR lacks miRNA binding sites had a concomitant increase in mCherry expression (Fig. 1b). This indicates that in the absence of miRNA targeting of the mCherry mRNA, the level of expression of eYFP is proportional to the level of expression of mCherry. However, in cells with one miR-20 site in the mCherry 3′ UTR, the eYFP fluorescence initially increases with virtually no corresponding increase in mCherry expression level (Fig. 1c). To capture this behavior quantitatively, we measured joint distributions of mCherry and eYFP levels in single cells, binned the single cell data according to their eYFP levels, and calculated the mean mCherry level in each eYFP bin (See Methods; Supplementary Fig. 1). We refer to this binned joint distribution as the transfer function. As suggested by the representative single cells shown in Fig. 1c, the transfer function shows a threshold-linear behavior in which the mCherry level, which represents the target protein production, does not appreciably rise until a threshold level of eYFP is exceeded.

Mathematical modeling suggests molecular titration is responsible for thresholding

We developed a mathematical model of miRNA-mediated regulation that could reproduce the nonlinearity in the above transfer function (Fig. 2). This model (Fig. 2a) is inspired by previous models[16] used to describe protein-protein titration[17] and small RNA (sRNA) regulation in bacterial systems[18]. It describes the concentration of free target mRNA (r) subject to regulation by miRNA (m) as a function of bare transcriptional activity in the absence of regulation by miRNA (r_0). We assume that only r can be translated into protein. Experimentally, we expect the mCherry signal to be proportional to the concentration of r, and the eYFP signal to be proportional to the concentration of r_0. The core of the model involves the binding of r to m to form a mRNA-miRNA complex r^* and the release of m from the complex back into the pool of active miRNA molecules either with or without the accompanying destruction of r. We assume that the total amount of miRNA is constant. Indeed, we observe no decrease in the miR-20 level beyond experimental uncertainty as a function of eYFP (Supplementary Fig. 2). The qualitative shape of the transfer functions generated by the model depends on two key lumped parameters. The first parameter λ, which behaves like a dissociation constant, governs the sharpness of the threshold (Fig. 2b). On a log-log plot relating r to r_0 (Fig. 2d) the increased sharpness manifests itself as a slope (which we refer to as the logarithmic gain) greater than 1, marking a sensitive transition connecting the branches of the transfer function of slope 1 that indicate little protein expression (below the transition) and nearly maximal protein production (above the transition). λ is inversely proportional to the rate at which miRNA binds the target mRNA (k_{on}); as k_{on} increases at a constant k_{off}, λ decreases and thus sharpens the transition. The threshold constant θ plays a role in the placement of the threshold and also in the sharpness of the transition between the threshold and escape regimes (Fig. 2c). θ is proportional to the

concentration of free miRNA available within the cell; as the total concentration of free miRNAs increases, θ increases and pushes the threshold to higher values of r_0 (Fig. 2e). We also considered a model that accounted for competition from the population of endogenous miRNA targets and found that including a pool of competing miRNA targets results simply in rescaling the θ and λ parameters characterizing the single target model (Supplementary Note).

The mathematical model thus suggests experiments that could be performed to modulate the thresholds generated by miRNA-mediated regulation. As our stable Tet-On HeLa cell lines could not achieve high enough levels of reporter expression to capture the complete sensitive transition to escape from miRNA-mediated repression, subsequent experiments were done by transiently transfecting Tet-On HeLa cells with reporter constructs and measuring fluorescence via flow cytometry to increase the number of cells in datasets. As with the quantitative fluorescence microscopy, we restrict our analysis to cells whose fluorescence is above cellular autofluorescence with at least, and in most cases greater than, 95% confidence.

Sharpening the threshold through addition of miR-20 binding sites

To sharpen the thresholds by increasing k_{on} we increased the number of miRNA binding sites *N* in the 3′ UTR of mCherry. The maximum logarithmic gain increases from approximately 1 when $N = 1$ to 1.8 when $N = 7$ (Fig. 3a); as expected from the model, the effect is stronger going from 1 to 4 binding sites than from 4 to 7 sites. We were also able to recapitulate a similar transfer function with $N = 7$ in the 3′ UTR of eYFP, thus isolating the effect to miR-20 mediated regulation rather than any property intrinsic to the mCherry reporter (Supplementary Fig. 3). Interestingly, unlike previous studies of bacterial sRNA[18], we can also directly test the importance of titration in generation of the threshold by using miR-20 binding sites that are perfectly complementary to the endogenous miR-20, thus converting the interaction between target and miRNA into a catalytic, RNAi-type repression. When the miR-20 bulged binding sites are replaced by a perfectly complementary binding site that yields the same maximum repression as $N = 7$ bulged sites, we do not observe gene expression thresholding (Fig. 3a, grey points).

To measure the fold repression as a function of target expression level, we measure for individual cells the transfer function in the absence of miR-20 binding sites and calculate the ratio of this control transfer function to transfer functions in the presence of 1, 4, and 7 miR-20 sites (Fig. 3b). As expected from Fig. 3a, increasing the number of binding sites increases the fold repression at lower eYFP levels, from just over 2-fold repression with a single miR-20 site to approximately 10-fold repression with seven miR-20 sites, while not significantly changing the fold repression at high eYFP (Fig. 3b). Seen this way, we demonstrate that rather than being only a subtle effect as suggested by population-based averages, which in this case results in at most 2.5-fold repression with seven binding sites (Fig. 3b, inset), regulation by miR-20 can exert very strong repression of protein production at low target transcript levels. Moreover the boundary of the regime of strongest repression is marked by a threshold level of transcription. Shifting this threshold to lower or higher

target mRNA levels by changing miRNA levels or number of binding sites can be of functional significance.

Shifting the threshold by modulating miR-20 abundance

Consistent with the model, the threshold can be shifted to either higher or lower eYFP levels by transfecting either miR-20 mimic oligonucleotides (siRNAs) or miRNA sponges that inhibit miR-20 activity[19] (Fig. 3c-d; Supplementary Fig. 4). Increasing the level of miRNA increased the fold repression below the threshold, increased the mRNA level needed to reach the threshold, and sharpened the transition. In the extreme case of seven miR-20 binding sites with 30 nM miR-20 mimic transfected (Fig. 3d), miRNA-mediated repression was ~40-fold as compared to a target with no miRNA binding site; the threshold was shifted to a 10-fold higher eYFP level; and the transition between repressed and unrepressed expression is quite sharp with a maximum logarithmic gain of ~5.4 (Fig. 3d), compared to ~1.8 without the transfected miR-20 mimic, i.e. endogenous levels (Fig. 3a). To quantitatively compare the data to the model, we simultaneously fit all the datasets holding λ constant across the fits for particular values of the constants N and θ for a particular amount of transfected siRNA mimic. Interestingly, the fit parameter θ, which recall is proportional to the concentration of miRNA available for target repression, increases with increasing siRNA mimic (Fig. 4a), but in a saturable fashion, while $1/\lambda$ increases linearly with N (Fig. 4b). The saturation suggests that the amount of transfected siRNA mimic entering functional complexes and thus available for target repression is limited, perhaps by entry into the cytoplasm and/or loading into Argonaute protein complexes.

Measuring gene expression thresholds in natural contexts

In order to test the generality of these findings, that the strength of repression of a miRNA target depends strongly on the relative amounts of the miRNA and its target, we sought to recapitulate the results in more physiological settings. First, we tested whether similarly sensitive transitions would be observed when the reporter construct incorporated naturally occurring miRNA binding sequences by fusing the 3′ UTRs of the oncogene *HMGA2* and the major GABA transporter gene *SLC6A1* to the mCherry reporter and performing dual-color flow cytometry. The *HMGA2* 3′ UTR contains seven binding sites for the miRNA family let-7, which is moderately expressed in HeLa cells, while *SLC6A1* contains three binding sites for the neuronal miRNA miR-218, which we supplied exogenously. The experiments showed that we could indeed observe sensitive transitions with these constructs (Fig. 5a,b). In addition, for *HMGA2* we increased the threshold incrementally by transfecting higher doses of let-7 siRNA mimic (Fig. 5a).

Finally we used a standard dual luciferase assay (see Methods, Supplementary Fig. 5) to measure target expression in mouse embryonic stem cells (ES cells) using only their endogenous pool of miRNA to retain physiological relevance. Here we measured a transfer function complementary to that in the experiments with HeLa cells: the mRNA target level remained fixed while the miRNA concentration varied. To test varying miRNA concentrations in ES cells we exploited the fact that different miRNA species are present at different abundances[20]. Finally, to gauge the strength of miRNA repression, target expression in wild-type ES cells was normalized to target expression in ES cells that lack the

enzyme Dicer and thus contain no miRNAs. We observe a similar threshold-linear behavior except that it reflects the level of miRNAs (Supplementary Fig. 5): at high miRNA abundances, repression is 5-fold but decreases with miRNA abundance until at the lowest miRNA levels target expression in wild-type cells is virtually indistinguishable from that in the miRNA-free $Dcr^{-/-}$ cells.

The threshold in regulation by miRNA is determined by the level of the miRNA and by the number and affinity of the target sites. Taking the case described above for regulation by endogenous miR-20 in HeLa cells, the threshold transition starts at approximately 60 target mRNAs per cell with seven typical sites in the 3′ UTR at an endogenous level of approximately 2,000 miR-20 molecules per cell (Supplementary Fig. 2, Supplementary Fig. 6). Many of these miRNAs as miRNP complexes could be bound to the endogenous miR-20 target mRNAs in the cell, leaving a limited pool for binding to the reporter mRNAs. Since these experiments are done at steady state conditions, this suggests that the miRNA system probably has limited capacity to accommodate increases in target populations. These results are consistent with our ability to strongly suppress miR-20 regulation of the target reporter by adding high levels of miR-20 target sites in the form of an exogenous sponge inhibitor[19] (Supplementary Fig. 4). The sponge phenomenon has been observed in multiple mammalian and non-mammalian organisms indicating its generality in miRNA regulation[21].

DISCUSSION

Our analysis of miRNA-mediated gene regulation at high target expression levels is consistent with previous population-based results, but measuring single cells offers a level of detail inaccessible to bulk assays. The detailed picture, which revealed a sensitive response of protein production to transcriptional activity bounded by strong repression at low target mRNA levels and weak repression at high target mRNA levels, may have important implications for miRNA-mediated regulation. There has been disparity between the concept of miRNAs as switches, exemplified by the *lin-14* developmental switch in *Caenorhabditis elegans* where there is a high degree of repression by the miRNA *lin-4*, versus many observations of miRNA-mediated regulation in mammalian cells where they are best considered as fine-tuners of gene expression. These results show that for some miRNA-target interactions, the miRNA behaves both as a switch, in the target expression regime below the threshold, and as a fine-tuner, in the sensitive transition between the threshold and the minimal repression regime at high mRNA levels.

The multi-site targets that we assayed are relevant to natural target genes because, though most target genes have only one conserved binding site for a given miRNA seed family, the majority of targets have sites for multiple miRNA families, with an average of more than four total conserved sites per 3′ UTR and many more poorly conserved sites[4]. This is further exemplified by the above results with targets containing natural miRNA sites from *HMGA2* and *SLC6A1*. In addition, we observed target reporter repression predominantly at the level of mRNA degradation (Supplementary Fig. 6d), as has been observed in genome-wide measurements of natural targets[22].

Our data and model suggest that the difference in repression between high and low target expression levels need not be inconsistent with the recently reported independence of the strength of repression of different target genes from their expression level[22]. Our results suggest that if the target pool of a miRNA is below the saturation regime, then all targets of a given affinity for the miRNA will be repressed to the same degree regardless of expression level. But if the target pool size grows, as it does when we introduce our reporter construct, then it is possible to saturate the pool of miRNAs. Our data and model are consistent with the dampening of the fold repression as target expression goes from low to high levels being due to a titration of the available cognate miRNA. This agrees with the observation that when the target contains a perfectly complementary site invoking an RNAi-type catalytic repressive mechanism, the threshold is abolished. Here there should be little stable titration of available miRNA. When a given miRNA target's abundance rises appreciably enough to titrate the miRNA, as we tested using sponge constructs, all the targets of that miRNA, not only the mCherry reporter, should experience derepression. These titration effects could also explain results from retrospective bioinformatic studies showing that a miRNA's overall target abundance negatively correlates with the miRNA's average repressive strength[23]. Mathematical modeling suggests that the pool of target mRNAs limits the ability of free miRNAs to bind to and repress additional targets (see Supplementary Note). In this regard, natural non-coding RNAs such as, potentially, pseudogene RNAs with UTR sequences matching those of protein-coding target genes[24] would also participate in this pool of competing molecules.

Gene expression thresholding may be an important feature of cell fate decisions. During a developmental transition where a tissue-specific miRNA is upregulated and its pool of target genes are down-regulated, a trend reported in fruitflies and in mammals,[25,26] the miRNA's effective concentration and therefore its potency could greatly increase. A target gene whose protein exerts its function at concentrations only above the threshold should exhibit a switch-like response. Switch-like derepression through molecular titration of miRNA could also enhance interactions within genetic networks. It has been shown that miRNAs often coordinately regulate targets that function together in pathways and protein complexes[27]. If the effect of the miRNA that targets such a gene network were sensitively switched off through titration, then the gene network could rapidly switch "on" in a coordinated manner.

METHODS

Reporter plasmid construction

Fluorescent reporters were cloned into pTRE-Tight-BI (Clontech). NLS sequences (ATGGGCCCTAAAAAGAAGCGTAAAGTC) were appended to the N-terminus of the eYFP and mCherry ORFs (Clontech) by PCR. The NLS-eYFP was inserted with EcoRI and NdeI. The NLS-mCherry was inserted with BamHI and ClaI. Regulatory elements were placed into the eYFP 3′ UTR with NdeI and XbaI; they were placed into the mCherry 3′ UTR with ClaI and EcoRV. $N = 1$ bulged miR-20 binding site (TACCTGCACTCGCGCACTTTA) was appended by PCR. $N = 4$ and $N = 7$ miR-20 sites, separated by CCGG spacers, were PCR-amplified from miR-20 sponge constructs (Ebert 2007). All constructs were sequence-confirmed. *HMGA2* wild type and seed-mutant 3′

UTRs[28] were a gift from Christine Mayr, David Bartel lab. The *SLC6A1* 3′ UTR fragment (nt 703–2041) was PCR-amplified from human genomic DNA.

Generation of stable lines

Reporter plasmids were linearized with AseI and cotransfected at 20:1 ratio with linear puromycin marker (Clontech). Transfected cells were selected in 2.5 μg/ml puromycin with 200 μg/ml G418. Individual eYFP-positive colonies were isolated, grown, and sorted for eYFP-positivity upon dox induction (MoFlo, DAKO-Cytomation).

Fluorescence microscopy

Cells were plated on glass-bottomed Nunc chambers (#1), and induced with dox for 4 days to ensure steady state reporter expression levels, Cell confluency was ~90 percent. This level of confluency was held constant between different constructs in any given experiment. Roughly 2,500 cells were imaged in a Nikon TEI-2000 inverted fluorescence microscope with a Princeton Instruments Pixis back-cooled CCD camera. Images were processed using custom software in MATLAB. Briefly, following subtraction of camera background and any cellular autofluorescence, pixel values in both eYFP and mCherry channels corresponding to cells expressing the construct were extracted. The single-cell data were then binned along the eYFP axis. Figure 1c reports the result of this binning procedure. In order to ensure that our measurements were within the dynamic range of our instruments, we only include data with a 95% confidence level above the autofluorescent background for analysis in both the fluorescence microscopy and flow cytometry experiments.

Transient transfection

Tet-On HeLa cells (Clontech) below passage 10 were plated in G418 (Gibco) 200 μg/ml and doxycycline (Sigma) 1 μg/ml media in 12-well dishes the day before transfection. Reporter plasmids were diluted 1:50 in pUC18b carrier plasmid (Qiagen HiSpeed maxipreps) and mixed with DreamFect Gold (Oz Biosciences), 8 μl reagent and 2 μg DNA per well. miR-20a, let-7b, and miR-218 mimics (Dharmacon) were cotransfected at the indicated concentrations. For U6 sponge assays, reporter plasmids were diluted 1:50 in sponge plasmid. Media was changed 24 hr post-transfection. Assays were performed 48 hr post-transfection. Reporter transfections were also performed with Lipofectamine 2000 (Invitrogen) with the same results.

Flow cytometry

Cells were run on LSRII analyzer (Becton Dickinson) with FACSDiva software. As above, cell confluency was ~90 percent. This level of confluency was held constant between different constructs in any given experiment. The raw FACS data were analyzed with FlowJo to gate cells according to their forward (FSC-A) and side (SSC-A) scatter profiles; specifically we chose cells near the peak of the (FSC-A, SSC-A) distribution. Untransfected cells were used to characterize the cellular autofluorescence in the LSRII analyzer from which we obtain the mean and standard deviation of the autofluorescence distribution. Each cell's eYFP and mCherry fluorescence values were subtracted by the mean autofluorescence plus twice the standard deviation. Following background subtraction, cells with eYFP

fluorescence levels less than 0 (i.e. indistinguishable from background) were excluded from further analysis and mCherry fluorescence levels less than 0 were set equal to 0. The single-cell data were then binned in the same manner as described above.

Fluorescence-activated cell sorting

Cells transfected with the $N = 0$ or $N = 7$ reporter were sorted 48 hr post-transfection into low and high fractions using a MoFlo high-speed sorting instrument (DAKO-Cytomation). Cell pellets were washed and snap-frozen before RNA isolation.

RT-PCR

Total RNA was harvested using RNeasy Micro Plus kit with the protocol modified for inclusion of small RNAs (Qiagen). RNA was treated with DNaseI (Ambion) and reverse-transcribed with oligo-dT primer using MMLV RTase (Ambion). qPCR for mCherry and eYFP was performed in triplicate reactions using SYBRGreen mix (Applied Biosystems), run on an Applied Biosystems 7500 Real-Time PCR instrument. Single-stranded DNA standards spiked into untransfected cell cDNAs were used for estimation of mCherry mRNAs per cell. miR-20 was measured with miScript RT-PCR assay (Qiagen) in quadruplicate reactions using miR-31 and snoRNA as controls.

Small RNA Northern blot

Total RNA was extracted from transfected cells with TRIzol (Invitrogen). 24 μg of total RNA was run on 12% polyacrylamide gel (UreaGel system, National Diagnostics), with miR-20 mimic as a standard, spiked into yeast sheared total RNA (Ambion). The blot was probed for miR-20a and $tRNA_{gln}$ as a loading control. Quantitation of bands was performed with ImageJ.

mES cell luciferase assays

Reporters were constructed by insertion of two bulged binding sites into the 3′ UTR of CMV Renilla luciferase. Cells were transfected in triplicate in 24-well plates with 2 μl Lipofectamine 2000 (Invitrogen), 0.01 μg of CMV-Renilla plasmid, 0.1 μg of pGL3 (Promega), and 0.69 μg of pWS (carrier plasmid). Cells were lysed and assayed 24 hr post-transfection by Dual Luciferase reporter assay (Promega) using a Glomax 20/20 luminometer (Promega).

Supplementary Material

Refer to Web version on PubMed Central for supplementary material.

Acknowledgments

This work was supported by an NIH Director's Pioneer Award to A.v.O. (1DP1OD003936) and the NIH/NCI Physical Sciences Oncology Center at MIT (U54CA143874); and by United States Public Health Service grants R01-CA133404 from the National Institutes of Health, PO1-CA42063 from the National Cancer Institute and partially by Cancer Center Support (core) grant P30-CA14051 from the National Cancer Institute (to P.A.S.). M.S.E. was supported by a HHMI Predoctoral Fellowship and a Paul and Cleo Schimmel Scholarship. G.X.Z. and J.S.T. were partially supported by Natural Sciences and Engineering Research Council of Canada Post Graduate Scholarships. We thank Gregor Neuert for help with cloning the reporter genes, Koch Institute flow cytometry staff for training and cell sorting, and David Bartel for helpful discussions.

References

1. Lewis BP, Burge CB, Bartel DP. Conserved seed pairing, often flanked by adenosines, indicates that thousands of human genes are microRNA targets. Cell. 2005; 120:15–20. [PubMed: 15652477]
2. Selbach M, et al. Widespread changes in protein synthesis induced by microRNAs. Nature. 2008; 455:58–63. [PubMed: 18668040]
3. Baek D, et al. The impact of microRNAs on protein output. Nature. 2008; 455:64–71. [PubMed: 18668037]
4. Friedman RC, Farh KK, Burge CB, Bartel DP. Most Mammalian mRNAs are conserved targets of microRNAs. Genome Res. 2009; 19:92–105. [PubMed: 18955434]
5. Lim LP, et al. The microRNAs of *Caenorhabditis elegans*. Genes Dev. 2003; 17:991–1008. [PubMed: 12672692]
6. Grimson A, et al. Early origins and evolution of microRNAs and Piwi-interacting RNAs in animals. Nature. 2008; 455:1193–1197. [PubMed: 18830242]
7. Yi R, Poy MN, Stoffel M, Fuchs E. A skin microRNA promotes differentiation by repressing 'stemness'. Nature. 2008; 452:225–229. [PubMed: 18311128]
8. Sluijter JPG, et al. MicroRNA-1 and -499 regulate differentiation and proliferation in human-derived cardiomyocyte progenitor cells. Arterioscler Thromb Vasc Biol. 2010; 30:859–868. [PubMed: 20081117]
9. Cimmino A, et al. miR-15 and miR-16 induce apoptosis by targeting Bcl2. Proc Natl Acad Sci USA. 2005; 102:13944–13949. [PubMed: 16166262]
10. Li X, Carthew RW. A microRNA mediates EGF receptor signaling and promotes photoreceptor differentiation in the Drosophila eye. Cell. 2005; 123:1267–1277. [PubMed: 16377567]
11. Bernstein E, et al. Dicer is essential for mouse development. Nat Genet. 2003; 35:215–217. [PubMed: 14528307]
12. Li X, Cassidy JJ, Reinke CA, Fischboeck S, Carthew RW. A microRNA imparts robustness against environmental fluctuation during development. Cell. 2009; 137:273–282. [PubMed: 19379693]
13. Li Y, Wang F, Lee JA, Gao FB. MicroRNA-9a ensures the precise specification of sensory organ precursors in Drosophila. Genes Dev. 2006; 20:2793–2805. [PubMed: 17015424]
14. Bagga S, et al. Regulation by let-7 and lin-4 miRNAs results in target mRNA degradation. Cell. 2005; 122:553–563. [PubMed: 16122423]
15. Raj A, van Oudenaarden A. Nature, nurture, or chance: stochastic gene expression and its consequences. Cell. 2008; 135:216–226. [PubMed: 18957198]
16. Elf J, Paulsson J, Berg OG, Ehrenberg M. Near-critical phenomena in intracellular metabolite pools. Biophys J. 2003; 84:154–170. [PubMed: 12524272]
17. Buchler N, Louis M. Molecular titration and ultrasensitivity in regulatory networks. J Mol Biol. 2008; 384:1106–1119. [PubMed: 18938177]
18. Levine E, Zhang Z, Kuhlman T, Hwa T. Quantitative characteristics of gene regulation by small RNA. PLoS Biol. 2007; 5:e229. [PubMed: 17713988]
19. Ebert MS, Neilson JR, Sharp PA. MicroRNA sponges: competitive inhibitors of small RNAs in mammalian cells. Nat Meth. 2007; 4:721–726.
20. Calabrese JM, Seila AC, Yeo GW, Sharp PA. RNA sequence analysis defines Dicer's role in mouse embryonic stem cells. Proc Natl Acad Sci USA. 2007; 104:18097–18102. [PubMed: 17989215]
21. Ebert MS, Sharp PA. MicroRNA sponges: progress and possibilities. RNA. in press.
22. Guo H, Ingolia NT, Weissman JS, Bartel DP. Mammalian microRNAs predominantly act to decrease target mRNA levels. Nature. 2010; 466:835–840. [PubMed: 20703300]
23. Arvey A, Larsson E, Sander C, Leslie CS, Marks DS. Target mRNA abundance dilutes microRNA and siRNA activity. Mol Sys Biol. 2010; 6:363.
24. Poliseno P, et al. A coding-independent function of gene and pseudogene mRNAs regulates tumour biology. Nature. 2010; 465:1033–1038. [PubMed: 20577206]

25. Stark A, Brennecke J, Bushati N, Russell RB, Cohen SM. Animal microRNAs confer robustness to gene expression and have a significant impact on 3′ UTR evolution. Cell. 2005; 123:1133–1146. [PubMed: 16337999]

26. Farh KK, et al. The widespread impact of mammalian microRNAs on mRNA repression and evolution. Science. 2005; 310:1817–1821. [PubMed: 16308420]

27. Tsang JS, Ebert MS, van Oudenaarden A. Genome-wide dissection of microRNA functions and cotargeting networks using gene set signatures. Mol Cell. 2010; 38:140–153. [PubMed: 20385095]

28. Mayr C, Hemann MT, Bartel DP. Disrupting the pairing between let-7 and Hmga2 enhances oncogenic transformation. Science. 2007; 315:1576–1579. [PubMed: 17322030]

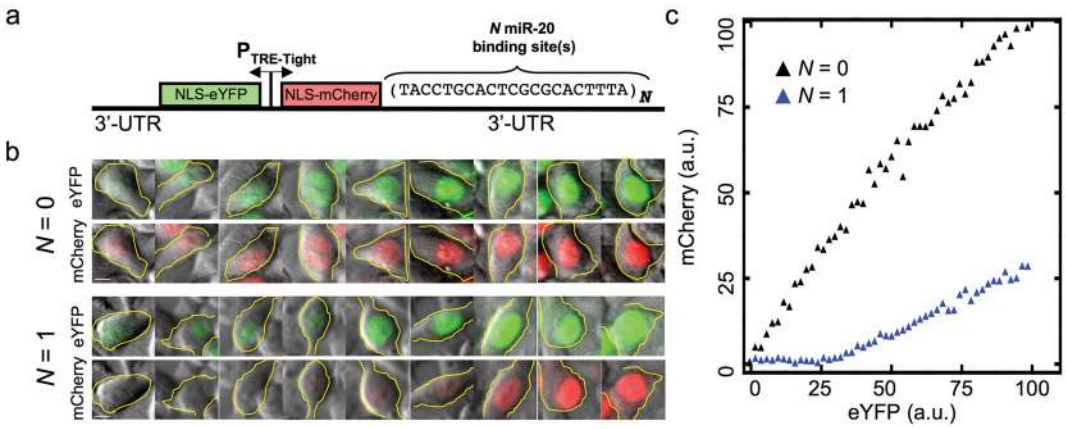

Figure 1.

Quantitative fluorescence microscopy reveals miRNA-mediated gene expression threshold. **(a),** The two-color fluorescent reporter construct consists of a bidirectional Tet promoter that co-regulates the enhanced yellow fluorescent protein (eYFP) and mCherry. Each fluorescent protein is tagged with a nuclear localization sequence (NLS) to aid in image analysis. The 3′ UTR of the mCherry gene is engineered to contain *N* binding sites for the miRNA mir-20. **(b),** Sample fluorescence microscopy data from representative single cells stably expressing eYFP and mCherry both in the presence and absence of regulation of mCherry by miR-20. The cells are arranged according to eYFP intensity. Scalebar is 5μm. **(c),** Transfer function relating eYFP to mCherry generated by binning according to eYFP intensity and plotting the mean mCherry in each bin. Supplementary Fig. 1 depicts a schematic of how the binning was performed on similarly structured flow cytometry data.

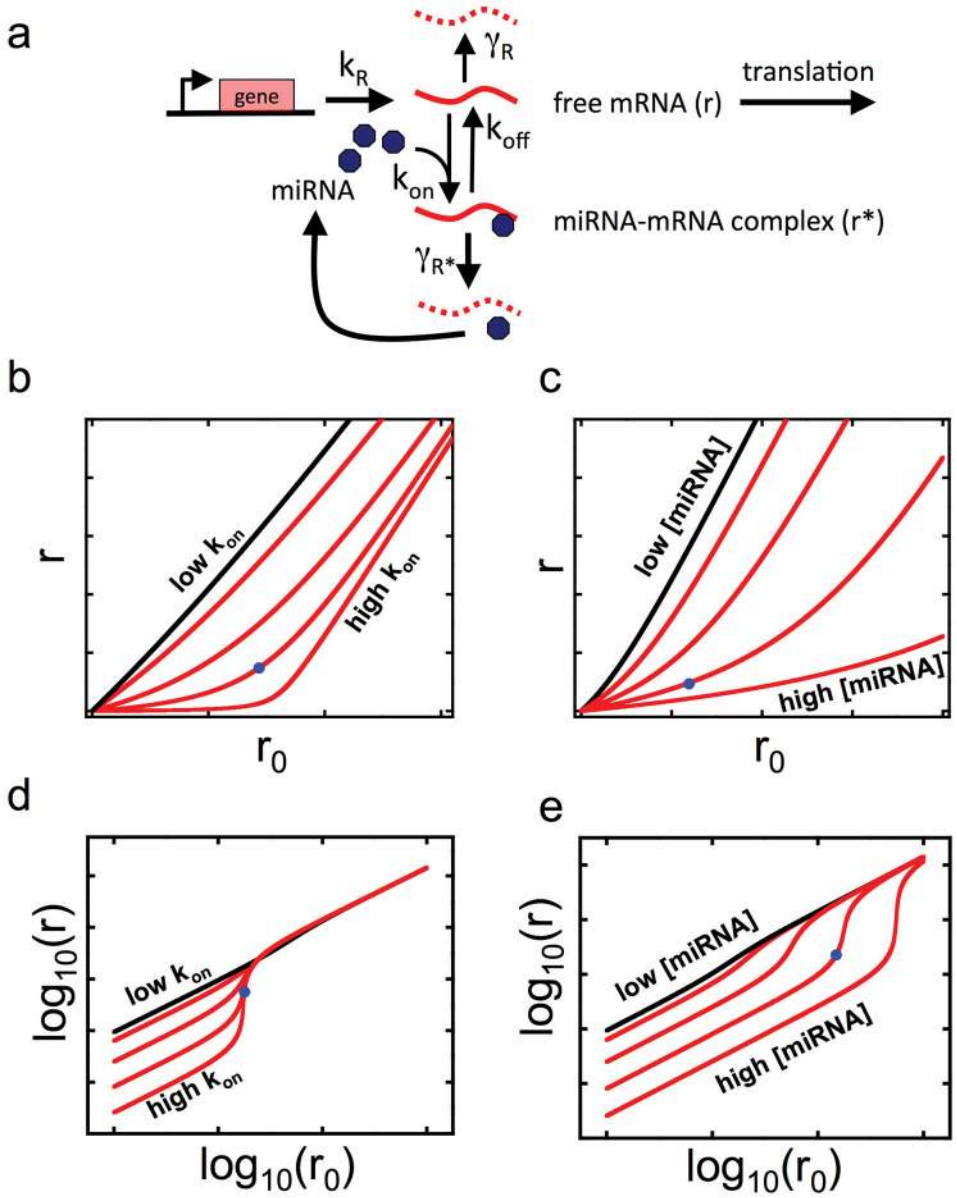

Figure 2.

Biochemical model of miRNA-mediated gene regulation. **(a),** The model describes the steady state level of mRNA free to be translated (*r*), which we experimentally observe as the mCherry signal, subject to regulation by miRNA (*m*) as a function of bare transcriptional activity in the absence of regulation by miRNA (r_0), which we experimentally observe as eYFP. The target mRNA is transcribed at a rate k_R and intrinsically decays with rate γ_R. miRNA and mRNA bind with rate k_{on} to form a complex (r^*). The bound miRNA can re-enter the pool of active miRNA either by unbinding the target mRNA with rate k_{off}, or destroying the mRNA with rate γ_{r*}. The steady state solution for *r* allows us to combine these microscopic parameters into two lumped parameters that govern the shape of the transfer function: λ, the effective dissociation constant characterizing the strength of the miRNA-mRNA interaction, and θ, proportional to the concentration of miRNA that acts on

the target mRNA. **(b),** Steady state solutions for r as a function of r_0 for various values of k_{on}; increasing k_{on} decreases λ. **(c),** Steady state solutions for r as a function of r_0 for various values of $[miRNA]_{total}$; increasing $[miRNA]_{total}$ increases θ. **(d),(e)** Same solutions as in (b) and (c) except depicted in log-log axes. The slope of the log-log curve is known as the logarithmic gain. Notably, thresholds in the linear representation appear as segments with logarithmic gain greater than 1 in the log-log representation. Increasing k_{on} increases the maximum logarithmic gain, but does not change its position along the r_0 axis, while increasing $[miRNA]_{total}$ increases the maximum logarithmic gain and shifts it to higher levels of r_0. Blue dots in panels (b)-(e) are guides to the eye to facilitate comparison between linear and logarithmic plots.

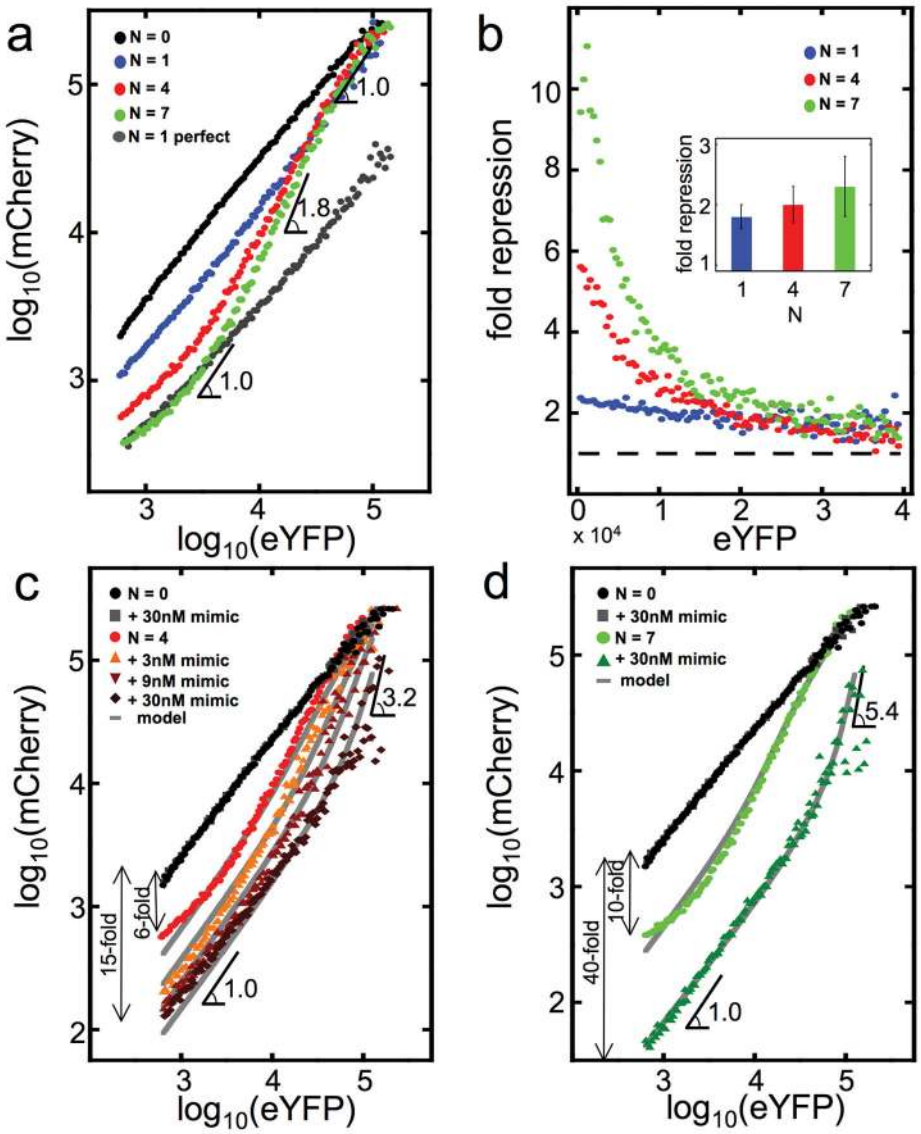

Figure 3.

Modulating the threshold. **(a),** Log-log transfer functions for $N = 0$, 1, 4, and 7. We can abolish the threshold by using a miR-20 binding site that is perfectly complementary to miR-20. **(b),** Ratio of $N = 0$ transfer function to $N = 1$, 4, and 7 transfer functions, depicting the fold repression as a function of eYFP expression. Inset depicts the average fold repression as a function of N. Using the flow cytometry data from panel (a), we compute the ratio of the mean eYFP level to the mean mCherry level for $N = 1$, 4, and 7. We then normalize this ratio by the mean eYFP to mean mCherry ratio for $N = 0$; we refer to this normalized ratio as the fold repression. Error bars are estimated by bootstrap sampling of the flow cytometry data. **(c),(d)** Effects of titrating defined amounts of miR-20 mimic siRNA on the transfer function for $N = 4$ (c) and $N = 7$ (d). In panels (a), (c), and (d) the angle symbol followed by a number denotes the value of the logarithmic gain, either minimum (when gain = 1) or maximum (when gain > 1).

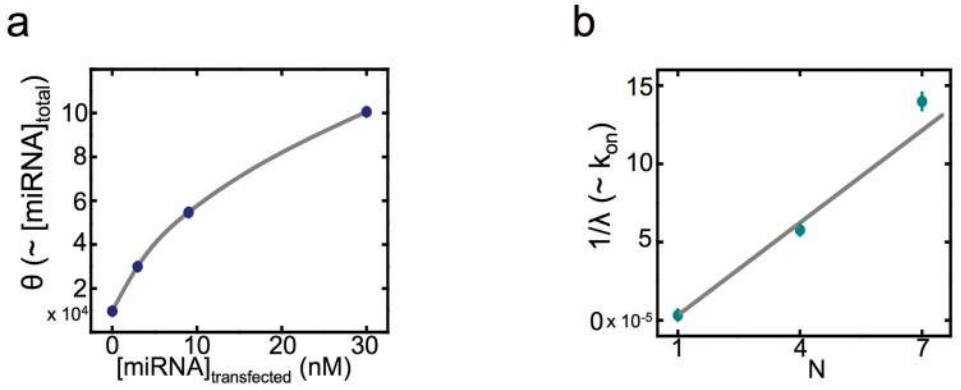

Figure 4.

(a),(b) Comparison to model. Following simultaneous fitting of all transfer function data to the quantitative model, the fitting parameter θ, proportional to the total amount of active miR-20 in the cell, is plotted against the amount of miR-20 mimic transfected (a); and 1/λ, proportional to the rate of mCherry-miR-20 association, is plotted against *N* (b).

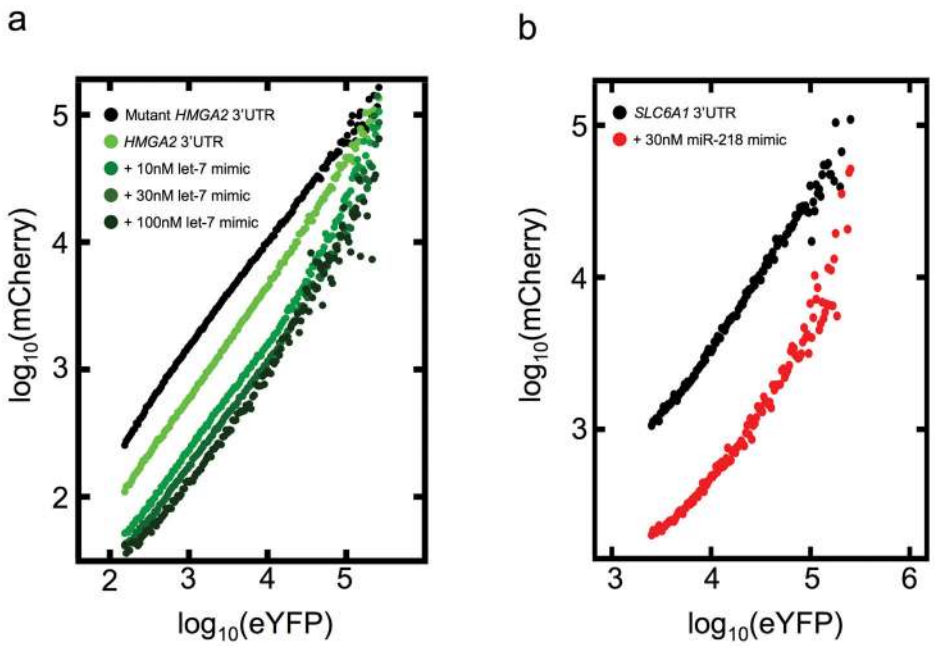

Figure 5.

Thresholding in endogenous 3′ UTRs. **(a)** The 3′ UTR of *HMGA2* or a version with the seven let-7 seed matches mutated was fused to mCherry. The reporters were cotransfected with varying concentrations of let-7b mimic. Cells were assayed by flow cytometry 48hr post-transfection. **(b)** The 3′ UTR of *SLC6A1*, which contains three seed matches for miR-218, was fused to mCherry. The reporter was transfected with or without miR-218 mimic. Cells were assayed by flow cytometry 48hr post-transfection.